

# Insight into primordial magnetic fields from 21-cm line observation with EDGES experiment

Teppei Minoda,<sup>1★</sup> Hiroyuki Tashiro,<sup>1</sup> and Tomo Takahashi<sup>2</sup>

<sup>1</sup>*Department of Physics and Astrophysics, Nagoya University, Nagoya 464-8602, Japan*

<sup>2</sup>*Department of Physics, Saga University, Saga 840-8502, Japan*

Accepted XXX. Received YYY; in original form ZZZ

## ABSTRACT

The recent observation of the 21-cm global absorption signal by EDGES suggests that the intergalactic medium (IGM) gas has been cooler than the cosmic microwave background during  $15 \lesssim z \lesssim 20$ . This result can provide a strong constraint on heating sources for the IGM gas at these redshifts. In this paper we study the constraint on the primordial magnetic fields (PMFs) by the EDGES result. The PMFs can heat the IGM gas through their energy dissipation due to the magnetohydrodynamic effects. By numerically solving the thermal evolution of the IGM gas with the PMFs, we find that the EDGES result gives a stringent limit on the PMFs as  $B_{\text{1Mpc}} \lesssim 10^{-10}$  G.

**Key words:** magnetic fields – cosmology: theory – dark ages, reionization, first stars

## 1 INTRODUCTION

In the Universe, there exist magnetic fields on a wide range of length scales  $L$ , from the planets (Connerney 1993) and stars (Donati & Landstreet 2009) with  $L \lesssim 1$  au, to the galaxy clusters (Carilli & Taylor 2002) and large-scale structure (Vacca et al. 2018) with  $L \gtrsim 1$  Mpc. Various observations have been revealing the nature of these magnetic fields (see also Han 2017; Han et al. 2018). However, the origin and evolution of large-scale magnetic fields are not understood yet and they are one of the challenging problems in modern cosmology (Durrer & Neronov 2013). Although the dynamo process might have played an important role in the amplification of large-scale magnetic fields (Brandenburg & Subramanian 2005), this mechanism cannot create magnetic fields from nothing. Therefore, many works study the possibility that the origin of these magnetic fields could be tiny magnetic fields created in some physical phenomena in the early universe, called the ‘primordial magnetic fields’ (PMFs). In the literature, the generation of the PMFs has been suggested in various cosmological epochs including the inflationary era (Turner & Widrow 1988; Ratra 1992), pre-heating (Bassett et al. 2001), phase transition (Hogan 1983; Quashnock et al. 1989; Baym et al. 1996; Anand et al. 2017), topological defects (Avelino & Shellard 1995; Sicutte 1997), the Harrison mechanism (Harrison 1970; Hutschenreuter et al. 2018), and so on (see, e.g., Kandus et al. 2011; Subramanian 2016 for reviews). Additionally, the possibility of the existence of the intergalactic magnetic fields with

$10^{-20}$ – $10^{-15}$  G has been argued by some previous works in this decade (Ando & Kusenko 2010; Neronov & Vovk 2010; Takahashi et al. 2013; Tashiro et al. 2014b), which motivates the study of the PMFs as the origin of magnetic fields in galaxy clusters and large-scale structure.

Constraints on the PMFs can provide the information on their generation mechanism and, moreover, give a hint to the physics of the early universe. So far, many constraints on the PMFs have been obtained from different cosmological observations: big bang nucleosynthesis (BBN) (Cheng et al. 1996), cosmic microwave background (CMB) temperature anisotropy (Planck Collaboration et al. 2016b) and its polarisation (Zucca et al. 2017), the CMB spectral distortion (Jedamzik et al. 2000; Kunze & Komatsu 2014), the baryon-to-photon number constraints between the BBN and the recombination epoch (Saga et al. 2018), the Sunyaev-Zel’dovich effect (Shaw & Lewis 2012; Tashiro & Sugiyama 2011; Minoda et al. 2017), the galaxy number count (Tashiro et al. 2010), the star formation history (Marinacci & Vogelsberger 2016), and so on.

Now the measurement of cosmological 21-cm line signatures is also expected to be a useful tool to constrain the PMFs. The 21-cm line signal depends on the physical states of neutral hydrogen gas such as its number density, its temperature and so on. The PMFs can provide the effect on them through the magnetohydrodynamic (MHD) effects (Sethi & Subramanian 2005). Tashiro & Sugiyama (2006) have pointed out that the measurements of 21-cm fluctuations by future radio interferometer telescopes can provide a strong constraint on the PMFs and have stimu-

★ E-mail: minoda.teppei@d.mbox.nagoya-u.ac.jp

lated further detailed studies (Shiraishi et al. 2014; Kunze 2019).

Bowman et al. (2018) have recently reported the detection of the strong radio absorption signal around 78 MHz with the Experiment to Detect the Global Epoch of Reionization Signature (EDGES). This result indicates that the gas temperature in the intergalactic medium (IGM) was cooler than the CMB temperature at the corresponding redshifts, i.e.,  $15 \lesssim z \lesssim 20$ . Therefore, the EDGES result can be interpreted as a constraint on a cosmological heating source. Note that the EDGES result is difficult to explain by the standard scenario: The amplitude of the absorption trough is almost twice as large as the maximal value expected in the standard cosmology. However, instead of giving an explanation on this anomaly, several authors have already applied the EDGES result to constrain some models: the Hawking evaporation of small primordial black holes (PBHs) (Clark et al. 2018), the emission from the accretion discs around large PBHs (Hektor et al. 2018), the decaying (Clark et al. 2018; Mitridate & Podo 2018) or annihilating dark matter (Cheng et al. 2018; D’Amico et al. 2018), warm dark matter (Safarzadeh et al. 2018), primordial power spectrum (Yoshiura et al. 2018) and so on.

In this work, we study the implication of the EDGES result to the PMFs and derive a constraint on them. The PMFs work as extra cosmological heating sources through the so-called ambipolar diffusion, in particular, in the late universe. Several authors have already pointed out that the measurement of the global 21-cm signal can put the constraint on the PMFs (Schleicher et al. 2009; Sethi & Subramanian 2009). Following these works, we evaluate the global thermal history with the PMFs and obtain a constraint on the amplitude and scale dependence of the PMFs.

This paper is organized as follows. In Section 2, we describe the time evolution of the 21-cm line signal, and we discuss the impact of the PMFs on it in Section 3. We report a constraint on the PMFs from the result of EDGES experiment in Section 4, and finally summarize our findings and discuss the future outlook in Section 5. In the analysis of this paper, we assume a flat  $\Lambda$ CDM model and fix cosmological parameters as obtained by Planck 2015 (Planck Collaboration et al. 2016a):  $\Omega_m = 0.308$ ,  $\Omega_b = 0.048$ ,  $h \equiv H_0/100 \text{ km s}^{-1} \text{ Mpc}^{-1} = 0.678$  where  $\Omega_m$  and  $\Omega_b$  are the density parameters for the matter and baryon and  $h$  is the reduced Hubble constant.

## 2 GLOBAL 21-CM LINE SIGNAL

In cosmological 21-cm line measurements, we observe the differential brightness temperature (Furlanetto et al. 2006),

$$\delta T_b(z) \approx 27 x_{\text{HI}}(z) \left[ 1 - \frac{T_\gamma(z)}{T_{\text{spin}}(z)} \right] \times \left( \frac{\Omega_b h^2}{0.02} \right) \left( \frac{0.15}{\Omega_m h^2} \right)^{1/2} \left( \frac{1+z}{10} \right)^{1/2} \text{ [mK]}, \quad (1)$$

where  $x_{\text{HI}}$  is the neutral fraction of hydrogen,  $T_\gamma$  is the CMB temperature and  $T_{\text{spin}}$  is the spin temperature defined by the population ratio of the hyperfine levels in a neutral hydrogen. Since we are interested in the global 21-cm line signal, all of these quantities are treated as background ones.

When the spin temperature is the same as the CMB one, the 21-cm signal vanishes as shown in equation (1). In the cosmological context, there are two processes to make the spin temperature deviate from the CMB one. One is the collisional interaction and the other is the interaction with Ly  $\alpha$  flux field (Wouthuysen 1952; Field 1959). They can couple the hyperfine structure with the IGM gas temperature. Besides the CMB interaction (the 21-cm photon emission and absorption), these processes control the evolution of the spin temperature. The spin temperature evolves between the values of the CMB and the IGM gas temperatures.

In the standard cosmology, the spin temperature evolution can be divided into four regimes. First, after the decoupling of the gas temperature from the CMB one around  $z \sim 200$ , the spin temperature follows the gas temperature through the collisional coupling. Then at the second stage, the spin temperature approaches to the CMB one because the collisional interaction becomes weak due to the cosmic expansion. In the third regime, the first luminous objects play important roles. They can produce a strong Ly  $\alpha$  field and Ly  $\alpha$  interaction becomes effective. So far the gas temperature evolves adiabatically after the decoupling from the CMB one and the gas is cooler than the CMB. Accordingly the spin temperature also gets lower than the CMB one. Equation (1) tells us that the global 21-cm signal becomes negative in this regime. In other words, the signals are observed as the absorption trough. After that, as the star and galaxy formation becomes active, a lot of ultraviolet (UV) photons are produced in this regime. They start to ionize and heat up the gas. Quickly the gas temperature increases and surpasses the CMB temperature. The spin temperature also becomes higher than the CMB and the signal is measured as emission. Gradually the IGM gas is ionized and, finally, the ionization of the IGM is completed. At this point the global 21-cm signal totally vanishes again.

Recently, the EDGES experiment has reported the absorption signal of global redshifted 21-cm lines between redshifts  $15 \lesssim z \lesssim 20$ . This result would indicate that the neutral hydrogen hyperfine structure coupled well with the gas temperature through Ly  $\alpha$  field and the gas temperature was lower than the CMB one around these redshifts. In the next section, we show how the PMFs affect the evolution of the IGM gas temperature.

## 3 THE FORMALISM OF THE PRIMORDIAL MAGNETIC FIELDS

Since our final aim is to constrain the strength and scale dependence of the PMFs, we provide their statistical properties. First, we assume the PMFs as statistically homogeneous and isotropic random Gaussian fields. The statistical property of such PMFs is completely determined by only the power spectrum,  $P_B(k)$ , as Landau & Lifshitz (1980)

$$\langle B_i^*(\mathbf{k}) B_j(\mathbf{k}') \rangle = \frac{(2\pi)^3}{2} \delta_D(\mathbf{k} - \mathbf{k}') (\delta_{ij} - \hat{k}_i \hat{k}_j) P_B(k), \quad (2)$$

where  $B_i^*(\mathbf{k})$  is a Fourier component of  $B_i(\mathbf{x})$  with a mode  $\mathbf{k}$  and we assume that the PMFs are non-helical fields.

For simplicity, we assume that the power spectrum of

the PMFs is given by the single power law in  $k$  space as

$$P_B(k) = \frac{(2\pi)^{n_B+5}}{\Gamma(\frac{n_B+3}{2})} B_n^2 \frac{k^{n_B}}{k_n^{n_B+3}} \quad (\text{for } k < k_{\text{cut}}). \quad (3)$$

Here, we set  $k_n \equiv 2\pi \text{ Mpc}^{-1}$  as a reference scale,  $B_n$  is the amplitude of the PMFs normalized at the length of 1 Mpc, and  $n_B$  gives the scale dependence. The case of  $n_B = -3.0$  corresponds to the scale-invariant PMFs and we adopt  $n_B > -3.0$  throughout this paper to avoid the infrared divergence of the PMFs and  $\Gamma(x)$  represents the gamma function.

On the other hand, in the UV regime, the PMFs have the cut-off scale due to the MHD effect in the early universe. According to previous studies (Jedamzik et al. 1998; Subramanian & Barrow 1998), the radiative diffusion before the recombination epoch damps the PMFs on small scales. The damping scale increases as the universe evolves. Therefore, we assume that the power spectrum has the sharp cut-off on the damping scale at the recombination epoch,

$$P_B(k) = 0 \quad (\text{for } k \geq k_{\text{cut}}). \quad (4)$$

We consider the time evolution of the cut-off scale as  $k_{\text{cut}}(t) = k_{\text{cut,init}} f(t)$  with  $f(t_{\text{init}}) = 1$ . Here  $k_{\text{cut,init}}$  is the cut-off scale at the initial time (the recombination epoch) as (Mack et al. 2002),

$$\left( \frac{k_n}{k_{\text{cut,init}}} \right)^2 = \frac{V_A^2}{\sigma_T} \int_0^{t_{\text{rec}}} \frac{dt}{a^2(t) n_e(t)} \approx \left[ 1.32 \times 10^{-3} \left( \frac{B_n}{1 \text{ nG}} \right)^2 \left( \frac{\Omega_b h^2}{0.02} \right)^{-1} \left( \frac{\Omega_m h^2}{0.15} \right)^{1/2} \right]^{\frac{2}{(n_B+5)}}, \quad (5)$$

where  $V_A$ ,  $\sigma_T$ ,  $n_e$  and  $t_{\text{rec}}$  are the Alfvén velocity, the cross-section for Thomson scattering, the electron number density, and the cosmic time at the recombination epoch, respectively. The time evolution of the cut-off scale is represented as  $f(t)$ . We will discuss the evolution  $f(t)$  later.

In constraining the PMFs, it is useful to introduce  $B_\lambda$ , which represents the field strength smoothed at any spatial length  $\lambda$ . By choosing the Gaussian window function in Fourier space,  $B_\lambda$  is related to  $B_n$  and  $k_\lambda = 2\pi/\lambda$  as<sup>1</sup>

$$B_\lambda^2 = \int_0^\infty e^{-k^2 \lambda^2} P_B(k) \frac{d^3 k}{(2\pi)^3} = B_n^2 \left( \frac{k_\lambda}{k_n} \right)^{n_B+3}. \quad (6)$$

After the recombination epoch, the magnetic fields dissipate their energy and heat the IGM gas through two processes (Sethi & Subramanian 2005). One is the decaying turbulence (DT) and the other is the ambipolar diffusion (AD). It has been shown that while the first one is active around the recombination epoch, the latter becomes effective at the late universe ( $z < 500$ ). The evolution of the IGM gas temperature  $T_K$  with the heating from the PMFs is given by

$$\frac{dT_K}{dt} = -2HT_K + \frac{x_e}{1+x_e} \frac{8\gamma\sigma_T}{3m_e c} (T_\gamma - T_K) + \frac{2}{3k_B n_b} (\dot{Q}_{\text{AD}} + \dot{Q}_{\text{DT}}), \quad (7)$$

<sup>1</sup> We have used this definition of the smoothed amplitude of the PMFs from Planck Collaboration et al. (2016b). Although this definition is slightly different from some other works (such as Fedeli & Moscardini 2012; Saga et al. 2018), the value of  $B_\lambda$  is almost unchanged among different definitions.

where  $H$ ,  $x_e$ ,  $\rho_\gamma$ ,  $m_e$ ,  $c$ ,  $k_B$  and  $n_b$  is the Hubble parameter, the ionization fraction of the baryon gas, the energy density of CMB photons, the rest mass of an electron, the speed of light, the Boltzmann constant, and the number density of the baryon gas, respectively.  $\dot{Q}_{\text{AD}}$  and  $\dot{Q}_{\text{DT}}$  on the right-hand side represent the global heating rate due to the ambipolar diffusion and the decaying turbulence, respectively. These two heating rates are written as (Sethi & Subramanian 2005)

$$\dot{Q}_{\text{AD}} = \frac{|(\nabla \times \mathbf{B}) \times \mathbf{B}|^2}{16\pi^2 \xi \rho_b^2} \frac{1-x_e}{x_e}, \quad (8)$$

$$\dot{Q}_{\text{DT}} = \frac{3w_B}{2} H \frac{|\mathbf{B}|^2}{8\pi} a^4 \frac{[\ln(1+t_d/t_{\text{rec}})]^{w_B}}{[\ln(1+t_d/t_{\text{rec}}) + \ln(t/t_{\text{rec}})]^{1+w_B}}, \quad (9)$$

with the time dependence of the decaying turbulence  $w_B \equiv 2(n_B+3)/(n_B+5)$ , the mass density of the baryon gas  $\rho_b$ , the physical time-scale for the decaying turbulence  $t_d$ , and the drag coefficient  $\xi = 1.9 (T_K/1 \text{ K})^{0.375} \times 10^{14} \text{ cm}^3 \text{ g}^{-1} \text{ s}^{-1}$  as referred to in Schleicher et al. (2008). Here, since we assume a blue spectrum of the PMFs,  $n_B > -3$ , we can take  $t_d = (k_{\text{cut}} V_A)^{-1}$  as the Alfvén time-scale at the cut-off scale of the PMFs, as referred to in Sethi & Subramanian (2005). Also, we can calculate the absolute value of the Lorentz force and the magnetic energy in equations (8) and (9) at a time  $t$  by substituting equation (3) with  $f(t)$  into  $|(\nabla \times \mathbf{B}) \times \mathbf{B}|^2 = \int (dk_1/2\pi)^3 \int (dk_2/2\pi)^3 k_1^2 P_B(k_1) P_B(k_2) f^{2n_B+8}(t)(1+z)^{10}$  and  $|\mathbf{B}|^2 = \int (dk/2\pi)^3 P_B(k) f^{n_B+3}(t)(1+z)^4$ . In this study, we neglect following two effects on the thermal evolution of the IGM gas included in the previous work (Schleicher et al. 2008). First, we do not take into account any radiative cooling effects, such as collisional excitation and ionization, recombination, and bremsstrahlung. We have confirmed these terms are negligible for the PMF model parameters of our interest. The other assumption is that there are no astrophysical objects. We mention this point in Section 5.

In order to solve equation (7), we also need to follow the evolution of the ionization fraction,

$$\frac{dx_e}{dt} = \gamma_e n_b x_e + \frac{1 + K_\alpha \Lambda n_b (1-x_e)}{1 + K_\alpha (\Lambda + \beta_e) n_b (1-x_e)} \times \left[ -\alpha_e n_b x_e^2 + \beta_e (1-x_e) \exp\left(-\frac{3E_{\text{ion}}}{4k_B T_\gamma}\right) \right], \quad (10)$$

where  $K_\alpha$ ,  $\Lambda$ ,  $\alpha_e$ ,  $\beta_e$  and  $\gamma_e$  are the parameters for the ionization and the recombination processes. For these parameters, we adopt the functions in Seager et al. (1999) and Seager et al. (2000) with the modifications suggested in Chluba et al. (2015). In equations (7) and (10), we neglect the primordial helium and the heavier elements for simplicity.

Finally, we comment on the time evolution of the cut-off scale  $f(t)$ . Since the dissipation of the PMFs is effective on smaller scales, the dissipation could evolve the cut-off scales. In this study, we obtain the evolution of  $f(t)$  based on the energy conservation of PMFs including the energy dissipation given in equations (8) and (9),

$$\frac{d}{dt} \left( \frac{|\mathbf{B}|^2}{8\pi} \right) = -4H \frac{|\mathbf{B}|^2}{8\pi} - \dot{Q}_{\text{AD}} - \dot{Q}_{\text{DT}}. \quad (11)$$

Rewriting this equations in terms of the PMF power spectrum with the cut-off scales, we can obtain the time evolution of  $f(t)$ .

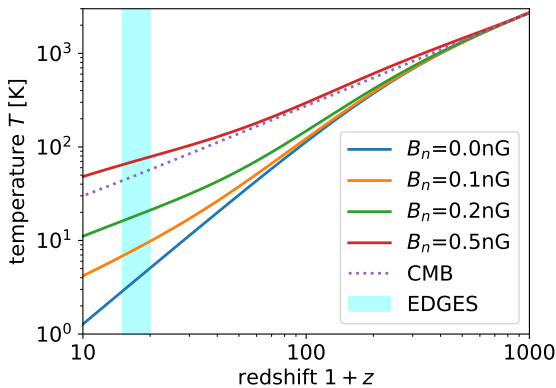


**Figure 1.** The gas temperature evolutions with the PMFs. The dotted line is the CMB temperature, and solid lines are the gas temperature for the cases with  $B_n = 0.0, 0.1, 0.2, 0.5$  nG, respectively. In this figure,  $n_B$  is fixed to  $-2.9$  for these lines. The blue shaded region represents the redshift range  $15 \lesssim z \lesssim 20$  corresponding to the strong absorption signal reported by EDGES.

Now, assuming the power spectrum of the PMFs, we solve equations (7), (10) and (11) simultaneously, and we can uniquely obtain the evolution of  $T_K$ ,  $x_e$ , and  $f(t)$  for a given PMF model with  $(n_B, B_n)$ .

#### 4 RESULTS

We show the evolution of the gas temperature  $T_K$  for different  $B_n$  with the nearly scale-invariant PMFs ( $n_B = -2.9$ ) in Fig. 1. Even with the sub-nano Gauss PMFs,  $T_K$  is strongly affected by the PMFs. In this case,  $T_K$  starts to be heated around  $z \sim 200$ , and is well deviated from the one in the case without the PMFs ( $B_n = 0$  nG).

We have confirmed that the ambipolar diffusion contributes to the heating of the IGM more than the decaying turbulence at the redshifts of our interest. Also the redshift dependence of the heating term in equation (8) follows as  $2\dot{Q}_{AD}/3k_B n_b \propto (1+z)$ . On the other hand, the dominant cooling term on the right-hand side of equation (7) for  $z \ll 200$  is the first one, and  $-2HT_K \propto (1+z)^{3.5}$ , which decreases faster than the heating term due to the ambipolar diffusion. Therefore, as we take larger values for  $B_n$ , the heating due to the ambipolar diffusion gets effective and dominates the cooling terms at higher redshifts. After the IGM is heated well and the magnetic energy is considerably dissipated, the heating source terms in equation (8) become decreased. As a result, the gas temperature starts to deviate from the adiabatic evolution ( $B_n = 0$  nG) at first, and the IGM is gradually getting cool after the saturation. We find the larger value of  $B_n$  makes the earlier and stronger heating, and the value of  $n_B$  determines the duration of the PMF heating.

The EDGES experiment has reported the detection of the global 21-cm absorption signals in the redshifts range  $15 \lesssim z \lesssim 20$  (Bowman et al. 2018). In Fig. 1 we highlight this redshift region with the blue shade. To create the absorption signal, the IGM gas temperature should be lower than the CMB temperature as shown in equation (1). Therefore, when the absorption signal is detected at the redshift  $z_{\text{abs}}$ , we can exclude a PMF parameter region  $(n_B, B_n)$  which gives

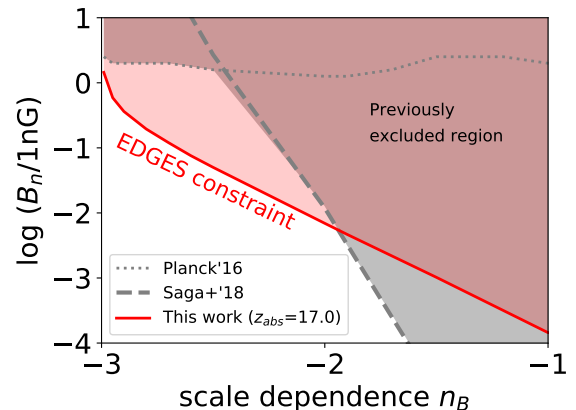


**Figure 2.** The upper limit of the PMFs parameters obtained by the recent observation of 21-cm line absorption by EDGES experiment (solid). The gray shaded region is the excluded region by previous works: Planck Collaboration et al. (2016b) in the dotted line and Saga et al. (2018) in the dashed line.

$T_K > T_\gamma$  at  $z_{\text{abs}}$ . According to the EDGES result, we set  $z_{\text{abs}} = 17$  which is the central redshift of the absorption signal in the EDGES experiment. Calculating the evolution of the gas temperature for different  $B_n$  with a fixed  $n_B$ , we get a novel constraint on the PMFs from the condition  $T_K < T_\gamma$  at  $z_{\text{abs}} = 17$ . The obtained constraints are  $B_n \lesssim 1.2 \times 10^{-1}$  nG for  $n_B = -2.9$ ,  $B_n \lesssim 6.3 \times 10^{-3}$  nG for  $n_B = -2.0$ , and  $B_n \lesssim 2.0 \times 10^{-4}$  nG for  $n_B = -1.0$ . We can fit our new constraint in a linear relation between  $B_n$  and  $n_B$  as

$$\log\left(\frac{B_n}{1 \text{ nG}}\right) \lesssim -\frac{(3n_B + 10)}{2} \quad \text{for } -3.0 < n_B < -1.0. \quad (12)$$

We plot our PMF constraint on the  $(n_B, B_n)$  plane in Fig. 2 with a solid line. For comparison, we also show the constraint from Planck Collaboration et al. (2016b) and the one from the magnetic reheating before the recombination (Saga et al. 2018) by the dotted and dashed lines, respectively. In the range of  $-3.0 < n_B < -2.0$ , the EDGES experiment could constrain the PMF amplitude most tightly.

Finally, by varying  $z_{\text{abs}}$  from 15 to 20, we have investigated the dependence of the PMF constraint on  $z_{\text{abs}}$ . We have found out that the resultant upper limit differs less than 10 per cent for different  $z_{\text{abs}}$  between 15 and 20. We can conclude that the dependence on  $z_{\text{abs}}$  is very weak.

#### 5 CONCLUSION

In this paper, we obtained a novel constraint on the PMFs from the result of the EDGES 21-cm global signal. The EDGES has reported the detection of the 21-cm absorption signals in the redshifts between  $15 \lesssim z \lesssim 20$ . This result suggests that the IGM gas is cooler than the CMB during this epoch. The PMFs can heat up the IGM gas by the dissipation of their energy through ambipolar diffusion and decaying turbulence. Therefore, the EDGES result can provide the constraint on the PMFs.

We have numerically evaluated the thermal evolution of the IGM gas with the PMFs. By requiring  $T_K < T_\gamma$  at  $z_{\text{abs}} = 17.0$  at which the EDGES absorption profile is centred,



we have obtained a stringent upper bound on the PMFs, roughly about  $B_n \lesssim 0.1$  nG. We also find that this PMF constraint is not changed very much if the absorption redshift is deviated from  $z_{\text{abs}} = 17.0$ .

To explain the EDGES anomaly, some non-standard cooling mechanisms are required, e.g. Tashiro et al. (2014a) and Barkana (2018). If we include such cooling in our analysis, our constraint on the PMFs should be relaxed. However, the IGM heating rates (equations 8 and 9) is proportional to  $B_n^4$  and  $B_n^2$ . Therefore, our constraint would not be modified very much even if we considered some non-standard cooling mechanisms.

To end this paper, we briefly discuss the impact of the astrophysical objects on the PMF constraint. Of course, they can significantly heat up and ionize the IGM gas, and the constraint from the 21-cm absorption signal might become tighter if we include such astrophysical processes (e.g. the star formation and the active galactic nucleus activity). On the other hand, some previous works have pointed out that the condition of the astrophysical object formation is also affected by the PMFs (Wasserman 1978; Shibusawa et al. 2014). In order to calculate the global 21-cm signal history with these effects, we should solve the fully non-linear MHD equations and the realistic astrophysical processes (Minoda et al. 2017; Kunze 2019). We leave these points to future work.

## ACKNOWLEDGEMENTS

We thank Kazuhiro Kogai, Hidenobu Yajima and Kenji Hasegawa for useful comments. This work is supported by KAKEN No. 15K17646 (HT), 17H01110 (HT) 15K05084 (TT), 17H01131 (TT) and MEXT KAKENHI Grant Number 15H05888 (TT).

## REFERENCES

- Anand S., Bhatt J. R., Pandey A. K., 2017, *J. Cosmology Astropart. Phys.*, **2017**, 051
- Ando S., Kusenko A., 2010, *ApJ*, **722**, L39
- Avelino P. P., Shellard E. P. S., 1995, *Phys. Rev. D*, **51**, 5946
- Barkana R., 2018, *Nature*, **555**, 71
- Bassett B. A., Pollifrone G., Tsujikawa S., Viniegra F., 2001, *Phys. Rev. D*, **63**, 103515
- Baym G., Bödeker D., McLerran L., 1996, *Phys. Rev. D*, **53**, 662
- Bowman J. D., Rogers A. E. E., Monsalve R. A., Mozdzen T. J., Mahesh N., 2018, *Nature*, **555**, 67
- Brandenburg A., Subramanian K., 2005, *Phys. Rep.*, **417**, 1
- Carilli C. L., Taylor G. B., 2002, *ARA&A*, **40**, 319
- Cheng B., Olinto A. V., Schramm D. N., Truran J. W., 1996, *Phys. Rev. D*, **54**, 4714
- Cheng H.-C., Li L., Zheng R., 2018, *Journal of High Energy Physics*, **9**, 98
- Chluba J., Paoletti D., Finelli F., Rubiño-Martín J. A., 2015, *MNRAS*, **451**, 2244
- Clark S. J., Dutta B., Gao Y., Ma Y.-Z., Strigari L. E., 2018, *Phys. Rev. D*, **98**, 043006
- Connerney J. E. P., 1993, *J. Geophys. Res.*, **98**, 18
- D’Amico G., Panci P., Strumia A., 2018, *Phys. Rev. Lett.*, **121**, 011103
- Donati J.-F., Landstreet J. D., 2009, *ARA&A*, **47**, 333
- Durrer R., Neronov A., 2013, *A&ARv*, **21**, 62
- Fedeli C., Moscardini L., 2012, *J. Cosmology Astropart. Phys.*, **11**, 055
- Field G. B., 1959, *ApJ*, **129**, 536
- Furlanetto S. R., Oh S. P., Briggs F. H., 2006, *Phys. Rep.*, **433**, 181
- Han J. L., 2017, *ARA&A*, **55**, 111
- Han J. L., Manchester R. N., van Straten W., Demorest P., 2018, *ApJS*, **234**, 11
- Harrison E. R., 1970, *MNRAS*, **147**, 279
- Hektor A., Hütsi G., Marzola L., Raidal M., Vaskonen V., Veermäe H., 2018, *Phys. Rev. D*, **98**, 023503
- Hogan C. J., 1983, *Phys. Rev. Lett.*, **51**, 1488
- Hutschenreuter S., Dorn S., Jasche J., Vazza F., Paoletti D., Lavaux G., Enßlin T. A., 2018, *Classical and Quantum Gravity*, **35**, 154001
- Jedamzik K., Katalinić V., Olinto A. V., 1998, *Phys. Rev. D*, **57**, 3264
- Jedamzik K., Katalinić V., Olinto A. V., 2000, *Phys. Rev. Lett.*, **85**, 700
- Kandus A., Kunze K. E., Tsagas C. G., 2011, *Phys. Rep.*, **505**, 1
- Kunze K. E., 2019, *J. Cosmology Astropart. Phys.*, **2019**, 033
- Kunze K. E., Komatsu E., 2014, *J. Cosmology Astropart. Phys.*, **1**, 009
- Landau L. D., Lifshitz E. M., 1980, *Statistical physics. Pt.1, Pt.2*
- Mack A., Kahnashvili T., Kosowsky A., 2002, *Phys. Rev. D*, **65**, 123004
- Marinacci F., Vogelsberger M., 2016, *MNRAS*, **456**, L69
- Minoda T., Hasegawa K., Tashiro H., Ichiki K., Sugiyama N., 2017, *Phys. Rev. D*, **96**, 123525
- Mitridate A., Podo A., 2018, *J. Cosmology Astropart. Phys.*, **5**, 069
- Neronov A., Vovk I., 2010, *Science*, **328**, 73
- Planck Collaboration et al., 2016a, *A&A*, **594**, A13
- Planck Collaboration et al., 2016b, *A&A*, **594**, A19
- Quashnock J. M., Loeb A., Spergel D. N., 1989, *ApJ*, **344**, L49
- Ratra B., 1992, *ApJ*, **391**, L1
- Safarzadeh M., Scannapieco E., Babul A., 2018, *ApJ*, **859**, L18
- Saga S., Tashiro H., Yokoyama S., 2018, *MNRAS*, **474**, L52
- Schleicher D. R. G., Banerjee R., Klessen R. S., 2008, *Phys. Rev. D*, **78**, 083005
- Schleicher D. R. G., Banerjee R., Klessen R. S., 2009, *ApJ*, **692**, 236
- Seager S., Sasselov D. D., Scott D., 1999, *ApJ*, **523**, L1
- Seager S., Sasselov D. D., Scott D., 2000, *ApJS*, **128**, 407
- Sethi S. K., Subramanian K., 2005, *MNRAS*, **356**, 778
- Sethi S. K., Subramanian K., 2009, *J. Cosmology Astropart. Phys.*, **11**, 021
- Shaw J. R., Lewis A., 2012, *Phys. Rev. D*, **86**, 043510
- Shibusawa Y., Ichiki K., Kadota K., 2014, *J. Cosmology Astropart. Phys.*, **8**, 017
- Shiraishi M., Tashiro H., Ichiki K., 2014, *Phys. Rev. D*, **89**, 103522
- Sicotte H., 1997, *MNRAS*, **287**, 1
- Subramanian K., 2016, *Reports on Progress in Physics*, **79**, 076901
- Subramanian K., Barrow J. D., 1998, *Phys. Rev. D*, **58**, 083502
- Takahashi K., Mori M., Ichiki K., Inoue S., Takami H., 2013, *ApJ*, **771**, L42
- Tashiro H., Sugiyama N., 2006, *MNRAS*, **372**, 1060
- Tashiro H., Sugiyama N., 2011, *MNRAS*, **411**, 1284
- Tashiro H., Takahashi K., Ichiki K., 2010, preprint, ([arXiv:1010.4407](https://arxiv.org/abs/1010.4407))
- Tashiro H., Kadota K., Silk J., 2014a, *Phys. Rev. D*, **90**, 083522
- Tashiro H., Chen W., Ferrer F., Vachaspati T., 2014b, *MNRAS*, **445**, L41
- Turner M. S., Widrow L. M., 1988, *Phys. Rev. D*, **37**, 2743
- Vacca V., et al., 2018, *MNRAS*, **479**, 776
- Wasserman I., 1978, *ApJ*, **224**, 337
- Wouthuysen S. A., 1952, *AJ*, **57**, 31

Yoshiura S., Takahashi K., Takahashi T., 2018, [Phys. Rev. D](#), **98**,  
[063529](#)  
Zucca A., Li Y., Pogosian L., 2017, [Phys. Rev. D](#), **95**, [063506](#)

This paper has been typeset from a  $\text{\TeX/L\AA\TeX}$  file prepared by the author.